IEICE TRANS. COMMUN., VOL. E81–B, NO. 9 SEPTEMBER 1998

PAPER

Real-Time CAC for ATM Multiple Service Categories Using Allan Variance

Masaki AIDA†, *Member*

SUMMARY This paper describes a real-time connection admission control scheme for supporting multiple service categories. The scheme is based on a real-time cell-loss ratio evaluation algorithm for VBR based on peak/sustainable cell rates and maximum burst size. The algorithm is based on a notion of Allan variance of VP utilization. The most remarkable characteristics of the admission control scheme are that it terminates within constant time, a few milliseconds, and that its time is independent of both the number of VCs and the capacity of a cell buffer.

key words: *ATM, CAC, service category, Allan variance*

1. Introduction

Asynchronous Transfer Mode (ATM) networks take advantage of the statistical behavior of sources with different traffic characteristics to efficiently share transmission resources through statistical multiplexing. Thus, they must be able to guarantee Quality of Service (QoS) for these types of traffic. To enable the support of different types of source traffic generated by a variety of applications, there are several service categories. QoS control schemes should support the individual service categories that are available through the ATM networks. Since, in general, the quality of a Virtual Channel (VC) is affected by other VCs in the same and in other service categories, traffic control should support multiple service categories. A Connection Admission Control (CAC) that supports multiple service categories is particularly important for guaranteeing QoS.

In the CAC model described in this paper, a user specifies a service category and anticipated traffic characteristics at the time a VC is set up by using a source traffic descriptor (Fig. 1). The CAC section of each Virtual Path (VP) determines whether the network resources for the VC are sufficient or not, based on QoS standards and traffic descriptors. If there are not enough network resources available, the VC is rejected. Otherwise, the VC is accepted.

A CAC should satisfy the following four requirements:

- It should be simple so as to reduce network cost.
- It should be fast enough to make real-time decisions.
- It should support ATM multiple service categories.
- It should enable efficient utilization of networks.

CAC schemes are categorized into two classes. One is CAC using measurements of the actual cell stream [15], [16]. The other is based only on traffic contract parameters [9], [12], [13]. The cost of CAC networks based on measurements of the actual cell stream becomes higher than that of CAC networks that are based only on traffic contract parameters, e.g., GCRA parameters [1]. This paper, thus, focuses on a CAC scheme based only on GCRA parameters.

Contract-parameter based CAC schemes [9], [12], [13] are simple and require relatively light-weight calculations. This characteristic is necessary for making real-time decisions. In addition, they can be easily extended to under an environment of multiple priority classes [9], [14]. This characteristic is necessary for supporting multiple service categories of ATM. However, since they assume a buffer-less model [9] or a long burst-length limit [3], [12], [13], they do not give efficient utilization of networks.

In previously published works [5], [6], the author proposed real-time CAC schemes suitable for an environment in which multiple service categories are available. These schemes are based on a real-time cell-loss ratio (CLR) evaluation algorithm, and can support Constant Bit Rate (CBR), both real-time and non-real-time Variable Bit Rate (VBR), Available Bit Rate (ABR),

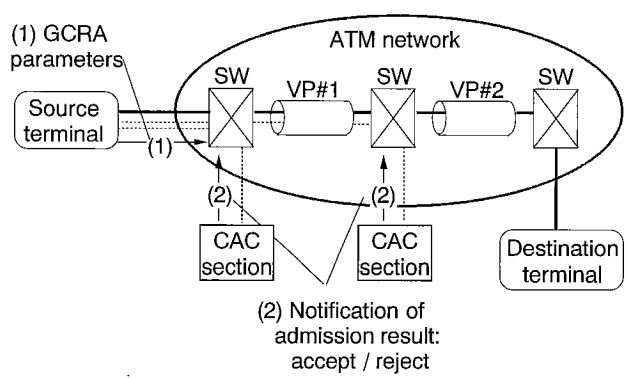

Fig. 1 Configuration of CAC sections.

Manuscript received December 22, 1997.
Manuscript revised March 11, 1998.

†The author is with Traffic Research Center, NTT Advanced Technology Corporation (NTT-AT), Musashino-shi, 180–0006 Japan.

and Unspecified Bit Rate (UBR) [2]. The most remarkable characteristics of these schemes are that they terminate within a few milliseconds and are independent of the number of VCs. However, in [5], [6], CLR evaluation processes of VBRs are based only on peak/sustainable cell rates (PCR, SCR), and this is valid only when the cell buffers have small capacity. Many recent major ATM applications, however, are data services and thus the cell buffers in ATM switches have large capacity. It is therefore necessary to take the buffer capacity and maximum burst size (MBS) into consideration in order to achieve efficient utilization of networks.

This paper describes a new CAC scheme that can take the relationship between the buffer capacity and MBS into consideration to achieve efficient utilization of networks. This scheme is an extension of the previously reported schemes [5], [6], and is based on an efficient real-time CLR evaluation algorithm [7]. The new CAC scheme satisfies each of the four requirements referred to earlier in this section.

This paper is organized as follows: In Sect. 2, we define the terminology and show the real-time CLR evaluation scheme used in this paper. Real-time CLR evaluation for each service category is explained in Sect. 3. Section 4 gives a framework of the real-time CAC scheme that supports multiple service categories. Finally, in Sect. 5, we show the efficiency of this scheme through numerical examples. The accuracy of CLR evaluation and the short processing time of the proposed CAC are also discussed.

2. Background

2.1 Terminology

Each transmission link can accommodate one or more VPs. Each VP is assumed to have a rigid boundary, or in other words, each VP is assigned a fixed bandwidth. The transmission link may be used as one VP. Each VC accommodated in the VP is assigned to one of several service categories.

In the current work, we divided time into fixed-length slots, each of which corresponds to an ATM cell's transmission time. The slot length is defined as L/C, where L is the cell length [bits] and C is the capacity of the VP [bps]. We adopt the slot length as a unit of time.

Each VC in the VP is indexed by i. Some important notations, used in this paper, are listed in Table 1.

Table 1 Notations.

Σ^c	Set of CBR VCs.
Σ^r	Set of real-time VBR VCs.
Σ^n	Set of non-real-time VBR VCs.
P_i	Peak Cell Rate (PCR) of the VC i. [cells/slot]
S_i	Sustainable Cell Rate (SCR) of the VBR VC i. [cells/slot]
B_i	Maximum Burst Size (MBS) of the VBR VC i. [cells]

2.2 Allan Variance of VP Utilization

Allan variance, originally introduced as a fluctuation index for the frequency of an atomic clock [8], is defined as the variance of finite-time average. It is closely related to spectrum analysis using the Fourier transformation [11].

Let us consider an observation of VP utilization during a time period t. The observed value, denoted as $X(t)$, is a finite-time average. If t is large, $X(t)$ is close to the real one $E[X]$. For small t, however, the observed value fluctuates around $E[X]$ in general. This is caused by burstiness of traffic. We describe the burstiness using Allan variance such as

$$E[(X(t) - E[X])^2],$$

where this is a function of t.

There are n VBR VCs in a VP. Then we have three parameters PCR P_i, SCR S_i, and MBS B_i for each VC i $(i = 1, 2, \ldots, n)$. We assume that the traffic characteristics of the VBR VCs comply with the GCRA specified by the ATM Forum [1].

For the worst case evaluation of Allan variance, source traffic of each VBR VC i is limited to satisfy the following three conditions:

- Actual maximum cell rate is PCR, P_i,
- Actual average cell rate is SCR, S_i, and
- For an arbitrary time t_0, the bursts with the maximum length at the PCR are always included in $t > t_0$. This means the bursts always included in the future traffic pattern.

We call the traffic patterns ceiling patterns, and define the set of all ceiling patterns as $\mathcal{S}_i$.

For a ceiling pattern $\varsigma \in \mathcal{S}_i$, we define the average utilization of the VP caused by the VBR VC i, and observed during successive time $[0, t)$, to be $X_i(t, \varsigma)$. Allan variance [4] of the VP utilization with respect to the VBR VC i is defined as

$$\sigma_i^2(t) := \sup_{\varsigma \in \mathcal{S}_i} E\left[(X_i(t, \varsigma) - S_i)^2\right]. \quad (1)$$

From [4], $\sigma_i^2(t)$ in asymptotic regions $t \ll 1$ and $t \gg 1$ can be evaluated by using only GCRA parameters of the VC i, and for $t \gg 1$,

$$\sigma_i^2(t) = \mathcal{O}(t^{-2}). \quad (2)$$

In the case that there is only one VC in the multiplexer, no deformation of traffic pattern occurs. Therefore, the Allan variance $\sigma_i^2(t)$ with respect to VC i is approximately expressed as

$$\sigma_i^2(t) = \begin{cases} S_i\,(1-S_i), & (t \leqq T_i), \\ \alpha_i\, t^{-2}, & (T_i < t), \end{cases} \tag{3}$$

where

$$\alpha_i = \inf\{\,\xi \mid \sigma_i^2(t)\, t^2 \leqq \xi\} \leqq \frac{1}{4} B_i^2, \tag{4}$$

$$T_i = \sqrt{\frac{\alpha_i}{S_i\,(1-S_i)}}. \tag{5}$$

Next, we consider Allan variance of the VP utilization $\sigma^2(t)$ with respect to all aggregated VBR VCs accommodated in the VP. From [4], asymptotic behaviors of $\sigma^2(t)$ are derived as follows: In the case of asymptotic region $t \ll 1$,

$$\sigma^2(t) = C_1(\Sigma)\,(1 - C_1(\Sigma)), \qquad (t \ll 1), \tag{6}$$

where Σ denotes a set of VBR VCs, and

$$C_1(\Sigma) := \sum_{i \in \Sigma} S_i. \tag{7}$$

In the case of asymptotic region $t \gg 1$,

$$\sigma^2(t) \leqq \alpha(\Sigma)\, t^{-2}, \qquad (t \gg 1), \tag{8}$$

where

$$\alpha(\Sigma) := \sum_{i \in \Sigma} \alpha_i \tag{9}$$

Hereafter, we assume, for the worst case, that (8) is an equality, and

$$\alpha(\Sigma) = \frac{1}{4} \sum_{i \in \Sigma} B_i^2. \tag{10}$$

The Allan variance $\sigma^2(t)$ is, therefore, approximately expressed as

$$\sigma^2(t) = \begin{cases} C_1(\Sigma)\,(1 - C_1(\Sigma)), & (t \leqq T(\Sigma)), \\ \alpha(\Sigma)\, t^{-2}, & (T(\Sigma) < t), \end{cases} \tag{11}$$

where

$$T(\Sigma) := \sqrt{\frac{\alpha(\Sigma)}{C_1(\Sigma)\,(1 - C_1(\Sigma))}}. \tag{12}$$

Here, let us briefly consider the physical meaning of the time $T(\Sigma)$. For simplicity, let us consider the situation where there is sufficient cell buffer capacity and no cell-loss occurs. In general, differing traffic patterns of input/output at a switch are caused by traffic pattern deformation at the multiplexer in the switch. Thus if we count the number of incoming/outgoing cells during a finite time interval t, the observed values are different.

If the input traffic patterns from these VCs are not deformed at the multiplexer, and are mutually independent, the Allan variance of the aggregated traffic is denoted as

$$\widetilde{\sigma}^2(t) = \begin{cases} \displaystyle\sum_{i \in \Sigma} S_i\,(1-S_i), & (t \leqq \widetilde{T}(\Sigma)), \\ \alpha(\Sigma)\, t^{-2}, & (\widetilde{T}(\Sigma) < t), \end{cases} \tag{13}$$

where

$$\widetilde{T}(\Sigma) = \sqrt{\frac{\alpha(\Sigma)}{\displaystyle\sum_{i \in \Sigma} S_i\,(1-S_i)}}. \tag{14}$$

However, an actual Allan variance of aggregated traffic is expressed as $\sigma^2(t)$ by including the effect of traffic deformation. Figure 2 shows an example of behaviors of $\sigma^2(t) \times t^2$ and $\widetilde{\sigma}^2(t) \times t^2$ with respect to t. Two times $T(\Sigma)$ and $\widetilde{T}(\Sigma)$ always satisfy

$$\widetilde{T}(\Sigma) \leqq T(\Sigma), \tag{15}$$

where equality is valid if and only if there is one VC in the multiplexer. The inequality is caused by the deformation effect of traffic. Note that, from approximations (11) and (13), $\sigma^2(t)$ and $\widetilde{\sigma}^2(t)$ are identical in $t > T$. We can interpret that this means T characterizes the maximum length of the busy period at the multiplexer.

2.3 Real-Time CLR Evaluation Algorithm for VBR

The real-time CLR evaluation algorithm studied in [3] gives an accurate upper-bound for CLR when only PCR and SCR of each VC are available. This upper-bound corresponds to a situation such that each VC has a very long burst with respect to the capacity of a cell buffer. The algorithm, therefore, can not take the relationship between MBS and the capacity of a cell buffer into consideration. This section shows a new real-time CLR evaluation algorithm taking the relationship between MBS and the capacity of a cell buffer into consideration. To this end, our approach is to extend the algorithm shown in [3] using Allan variance, but then the characteristic of real-time calculation is retained in a new algorithm. In this section, we show a real-time CLR evaluation algorithm shown in [7] in a form suitable for extension to that for multiple service categories. Basic concepts of the extension are as follows:

- It includes a modification of PCR to appropriate value using SCR, MBS and the capacity of a cell buffer.

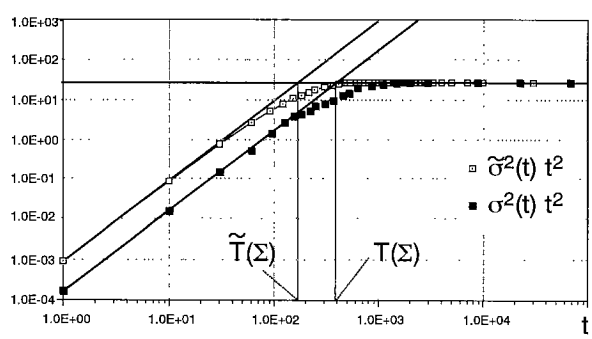

Fig. 2 Behaviors of $\sigma^2(t)$.

- In order to correct the number of lost cells, it uses an evaluation of the maximum length of busy periods at the multiplexer obtained from characteristics of Allan variance.

For VBR VCs, let us define the following parameters:

$$C_2(\Sigma,\Gamma) := \sum_{i\in\Sigma} S_i\,(\widetilde{P}_i(\Gamma) - S_i), \tag{16}$$

$$C_3(\Sigma,\Gamma) := \sum_{i\in\Sigma} S_i\,(\widetilde{P}_i(\Gamma) - S_i)\,(\widetilde{P}_i(\Gamma) - 2S_i), \tag{17}$$

where

$$\widetilde{P}_i(\Gamma) := \begin{cases} P_i, & (\Gamma P_i < B_i), \\ \dfrac{B_i}{\Gamma} + S_i\,\dfrac{\Gamma P_i - B_i}{\Gamma P_i}, & (\Gamma P_i \geq B_i), \end{cases} \tag{18}$$

and Γ is a constant such that

$$\Gamma := K + 1, \tag{19}$$

when the output buffer in an ATM switch has K cell places. Physical meanings of these parameters are as follows: $\Gamma\,\widetilde{P}_i$ denotes the maximum number of arriving cells during a Γ-slot interval. So, $\widetilde{P}_i$ is a cell rate which is the ratio of the maximum number of arriving cells during a Γ-slot interval to Γ. In order to take MBS and the buffer capacity into consideration, we modify P_i to $\widetilde{P}_i$. C_2 and C_3 mean normalized values of the second and the third cumulants of the number of arriving cells during a Γ-slot interval [3]. In this connection, C_1 of Eq. (7) means the first cumulant of the number of arriving cells during a Γ-slot interval. In addition, we define

$$C_L := \frac{-F_N + \sqrt{F_N^2 + G_N}}{2H_N(N+1)}, \tag{20}$$

where

$$H_N = 1 - \frac{1+\sqrt{3-2/N}}{N-1}, \tag{21}$$

$$F_N = C_2\,H_N\,(1-C_1), \tag{22}$$

$$G_N = 4\,C_2^3\,H_N\,(1-H_N)\,(N+1), \tag{23}$$

and $N\,(\geq 4)$ is the number of iterations determined from the target termination time for the calculation. From C_3 and C_L, we define D as

$$D := \max(C_3, C_L). \tag{24}$$

Thus, we obtain CLR evaluation B in the form

$$B(\Sigma,\Gamma) = \frac{R}{C_1}\exp(-A/R) \times \sum_{k=0}^{N-1} (M - \Lambda + k)\frac{(A/R)^{M+k}}{(M+k)!}, \tag{25}$$

where

$$R := \frac{D}{C_2},\quad A := \frac{C_2^2}{D},\quad \delta A := C_1 - A, \tag{26}$$

and, using $T(\Sigma)$, the maximum length of busy period obtained from the Allan variance,

$$\Lambda = \frac{1+\min(1,\Gamma/T(\Sigma))\,(1-C_1) - \delta A}{R},\quad M = \lceil \Lambda \rceil, \tag{27}$$

where $\lceil x \rceil$ denotes the minimum integer greater than or equal to x. Here, the physical meaning of Λ is a factor for correcting VP capacity. If busy period $T(\Sigma)$ is much longer than the capacity of a buffer, then $\Gamma/T(\Sigma) \cong 0$ and it is reduced to

$$R\,\Lambda = 1 - \delta A,$$

the same as in [3]. This is the case for long burst-length limit based only on PCR and SCR or for small buffer-capacity limit. In this case, if the number of cells arriving during a Γ-slot interval is greater than Γ, arriving cells exceeding Γ are considered to be lost. In general, however, although the number of cells arriving during a Γ-slot interval exceeds Γ, all of the those cells are not lost. $\min(1,\Gamma/T(\Sigma))\,(1-C_1)$ in (27) describes how many cells can be carried forward to the next Γ-slot interval.

In the CLR evaluation formula (25), however, it is necessary to calculate the factorial. This can be done by using Stirling's law,

$$\log m! \cong (m+1/2)\log m - m + (1/2)\log 2\pi. \tag{28}$$

Formula (25) gives a sufficiently accurate evaluation for CLR [7]. Since formula (25) is in the same mathematical form as the previous studied real-time CLR evaluation in [3], the calculation time is constant and is independent of both the number of VCs and the capacity of the cell buffer. Formula (25) can be calculated using four parameters, $C_1(\Sigma)$, $C_2(\Sigma)$, $C_3(\Sigma)$, and $\alpha(\Sigma)$. Calculation of these parameters requires only a minimal amount of processing because these values can be updated from previous values by applying a small number of addition and subtraction operations.

3. CLR Evaluation for Individual VBR Category

3.1 Transmission Discipline of Cell Buffers

To support multiple service categories, it is necessary to choose a transmission discipline at the output cell buffer in an ATM switch. For easy implementation, we chose a simple transmission discipline. This discipline should support the five service categories: CBR, real-time VBR (VBR-RT), non-real-time VBR (VBR-NRT), ABR, and UBR. We assign a cell buffer to each service category (Fig. 3) and assign deterministic capacity to each buffer.

Each buffer has a priority class for transmitting cells which corresponds to its service category. Cells

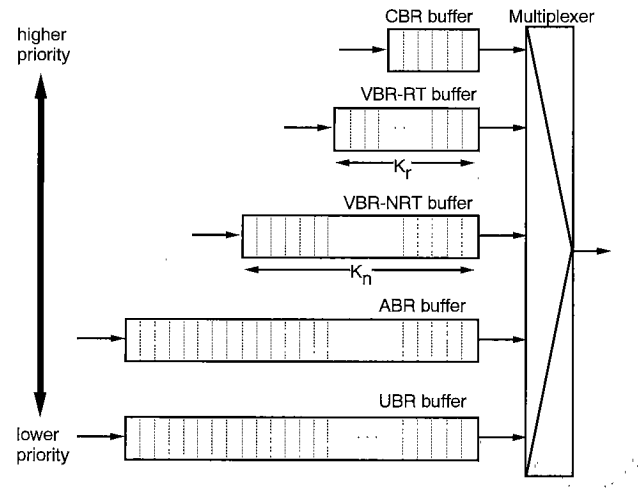

Fig. 3 Cell buffers in SW.

in one buffer can be transmitted only when there are no cells waiting in a higher priority buffer. CBR has the highest priority, followed by VBR-RT, VBR-NRT, ABR, and UBR. This type of priority control is easy to implement.

In this paper, we do not consider the QoS of the best-effort classes (ABR, UBR). Hence, the CAC corresponding to the best-effort classes always accepts required connections, and it is not included in the reminder of this paper. In case of ABR, if support with a non-zero minimum cell rate (MCR) is required, it is necessary for evaluating the available bandwidth for ABR. It is easy to extent and described in [6].

3.2 CLR Evaluation for VBR-RT

This section explains the real-time CLR evaluation for VBR-RT. The concept behind the CLR evaluation for VBR-RT is simple: Since CBR is the only service category that has a higher priority than VBR-RT, we only need to consider CBR and VBR-RT cells. Let the capacity of VBR-RT's cell buffer be K_r. We consider a single cell-buffer model with capacity K_r. Our approximation technique is to first calculate the CLR of the single buffer for the combined cell flow of CBR and VBR-RT. Then, we regard all the lost cells are belonging to VBR-RT, and CLR is isolated for only VBR-RT VCs from the mixed CLR. Concept of the approximation technique is same as in [5], [10]

To evaluate the CLR for VBR-RT using the CLR evaluation algorithm mentioned in the previous section, we set the parameters as follows:

$$\Gamma_r = K_r + 1. \tag{29}$$

For VBR-RT VCs, $\widetilde{P}_i$ must be calculated using Γ_r.

Since we take both CBR and VBR-RT VCs into account,

$$C_1(\Sigma^c \cup \Sigma^r). \tag{30}$$

Since there are no effects from CBR VCs, C_2 and C_3 are calculated using only VBR-RT VCs such that

$$C_2(\Sigma^c \cup \Sigma^r, \Gamma_r) = C_2(\Sigma^r, \Gamma_r), \tag{31}$$

$$C_3(\Sigma^c \cup \Sigma^r, \Gamma_r) = C_3(\Sigma^r, \Gamma_r). \tag{32}$$

By putting these parameters into (25), the CLR evaluation for VBR-RT B_r is obtained as

$$B_r = \frac{C_1(\Sigma^c \cup \Sigma^r)}{C_1(\Sigma^r)} B(\Sigma^c \cup \Sigma^r, \Gamma_r). \tag{33}$$

3.3 CLR Evaluation for VBR-NRT

This section explains the real-time CLR evaluation for VBR-NRT. Since both CBR and VBR-RT have higher priorities than VBR-NRT, it is necessary to take CBR, VBR-RT, and VBR-NRT cells into account. CBR cells have the highest priority and VBR-RT cells have priority over the rest of the bandwidth. The remaining bandwidth, i.e., not used by CBR and VBR-RT, can be used by VBR-NRT cells. Let the capacity of VBR-NRT's cell buffer be K_n. We consider a single cell-buffer model with capacity K_n. Similar to the VBR-RT case, we first calculate the CLR of the single buffer for the combined cell flow of CBR, VBR-RT and VBR-NRT. Then all the lost cells are regarded as belonging to VBR-NRT, and CLR is isolated for only VBR-NRT VCs from the mixed CLR.

To evaluate the CLR for VBR-NRT using the CLR evaluation algorithm, we set the parameters as follows:

$$\Gamma_n = K_n + 1. \tag{34}$$

For VBR-NRT VCs, $\widetilde{P}_i$ must be calculated by using Γ_n.

Since we take CBR, VBR-RT, and VBR-NRT VCs into account,

$$C_1(\Sigma^c \cup \Sigma^r \cup \Sigma^n). \tag{35}$$

Since there are no effects from CBR VCs, C_2 and C_3 are calculated by using only VBR-RT and VBR-NRT VCs as

$$C_2(\Sigma^c \cup \Sigma^r \cup \Sigma^n, \Gamma_n) = C_2(\Sigma^r \cup \Sigma^n, \Gamma_n), \tag{36}$$

$$C_3(\Sigma^c \cup \Sigma^r \cup \Sigma^n, \Gamma_n) = C_3(\Sigma^r \cup \Sigma^n, \Gamma_n). \tag{37}$$

By putting these parameters into (25), the CLR evaluation for VBR-NRT B_n is obtained as

$$B_n = \frac{C_1(\Sigma^c \cup \Sigma^r \cup \Sigma^n)}{C_1(\Sigma^n)} B(\Sigma^c \cup \Sigma^r \cup \Sigma^n, \Gamma_n). \tag{38}$$

4. CAC for Multiple Service Categories

This section explains the whole framework of real-time CAC for multiple service categories and each CAC algorithm corresponding to service category based on the real-time CLR evaluation.

4.1 Framework

The CAC section, corresponding to a VP, maintains the information of the service category and traffic descriptors of VCs already connected through the VP. Figure 4 illustrates the framework of a CAC section for supporting multiple service categories. At the time the VC is set up, the CAC section, corresponding to VPs on the potential route, obtains information, from the new VC, on the service category and traffic descriptor. Each CAC section checks the service category of the new VC and assigns it to a CAC algorithm corresponding to its service category (Fig. 4).

The CAC algorithm determines whether the new VC should be accepted or rejected based on the real-time CLR evaluations. The VC is accepted if and only if all CAC sections on the route can accept the VC, otherwise it is rejected. The user is notified of the result.

The CAC decision-making process in each CAC section is explained in the sections below.

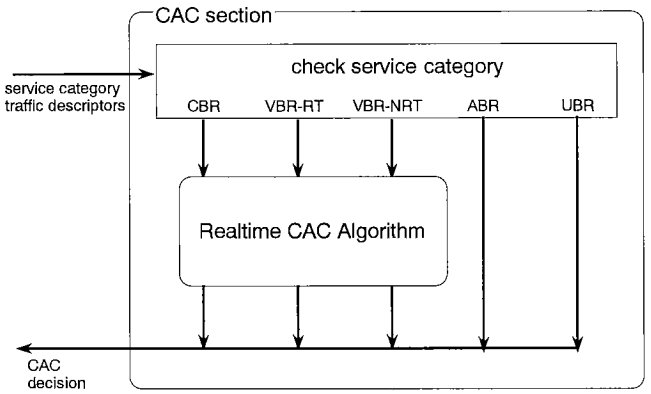

Fig. 4 Framework of a CAC section.

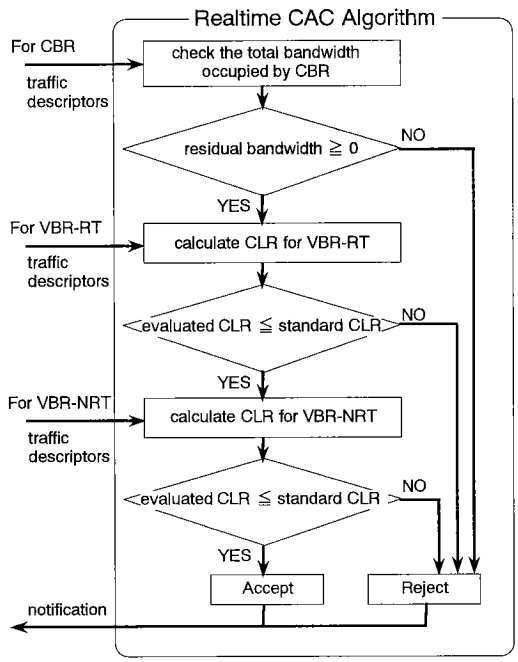

Fig. 5 Real-time CAC algorithm for each service category.

4.2 CAC Algorithm for VBR-NRT

When the new VC must to be set up is in VBR-NRT, the CAC algorithm for VBR-NRT calculates only the CLR evaluation for VBR-NRT as shown in Sect. 3.3.

If the evaluated CLR for VBR-NRT is smaller than or equal to the standard CLR, the new VC is accepted. Otherwise, the VC is rejected (Fig. 5).

4.3 CAC Algorithm for VBR-RT

If the VC has to be set up in VBR-RT, the CAC algorithm for VBR-RT calculates the CLR evaluations for VBR-RT and VBR-NRT as shown in Sects. 3.2 and 3.3. This is because the VC influences not only VBR-RT VCs but also VBR-NRT VCs. Even if the new VC has a higher priority than VBR-NRT VCs with respect to cell transmission, the new VC must not violate the QoS of VBR-NRT VCs that are already set up.

If the evaluated CLRs for VBR-RT and for VBR-NRT are smaller than or equal to the standard CLRs for VBR-RT and VBR-NRT, respectively, the new VC is accepted. Otherwise, the VC is rejected (Fig. 5).

4.4 CAC Algorithm for CBR

When the new VC is in CBR, the CAC algorithm for CBR calculates the CLR evaluations for VBR-RT and VBR-NRT as shown in Sects. 3.2 and 3.3. In addition, the CAC algorithm checks the total bandwidth occupied by CBR. The reason for these procedures is the same as that in the VBR-RT case.

If the total bandwidth occupied by CBR VCs including the new VC is smaller than or equal to the capacity of VP, the CAC algorithm calculates the CLR evaluations for VBR-RT and VBR-NRT. Otherwise, the new VC is rejected. Next, if the evaluated CLRs for VBR-RT and for VBR-NRT are smaller than or equal to the standard CLRs for VBR-RT and VBR-NRT, respectively, the new VC is accepted. Otherwise, the VC is also rejected (Fig. 5).

5. Numerical Examples

This section examines both the accuracy of our CLR evaluations and the processing time for the proposed CAC.

5.1 Accuracy of the CLR Evaluation Formula

Here we show the accuracy of evaluation formula (25) by comparing some evaluations with simulation results.

For a single priority class, CLR evaluation (25) gives a sufficiently accurate evaluation as shown in [7].

Here, we examine the CLR evaluation of lower priority cases (33) and (38) under an environment of multiple priority classes.

We compare the CLR evaluations and simulation results under the following conditions: There are two types of VCs, VC1 and VC2, where

- VC1: PCR = 25 Mbps, SCR = 5 Mbps, MBS = 50 cells,
- VC2: PCR = 10 Mbps, SCR = 2 Mbps, MBS = 100 cells,

in a 150-Mbps VP. Mixture ratios of the number of VC1 VCs to that of VC2 VCs are 1 : 1, 1 : 2, and 2 : 1. There are two priority classes and one of the above VC types is assigned priority. The transmission discipline is the same as shown in Fig. 3. The capacities of high-priority and low-priority buffers are 500 and 1000 cell places, respectively.

We compare CLR evaluations for lower priority VCs using Eq. (33) or (38) with simulation. The traffic model for each VC, used in the simulation, is an ON-OFF process modulated by a Markovian process, such that the cell rate during the ON-period is PCR, the cell rate during the OFF-period is 0, the average number of cells in the ON-period is equal to MBS, and the average length of OFF-period is determined by the average cell rate to be SCR.

Figures 6 (a) and (b) show CLR evaluations when the mixture ratio of VCs is 1 : 1. VC1 has priority in (a) and VC2 has priority in (b). The horizontal axis denotes VP utilization, and the vertical axis denotes evaluated and simulated CLRs for the lower-priority class. Although for smaller CLRs, the gap between the proposed evaluation method and the simulation result appears to be significant, the gap in utilization is small and the proposed CAC gives conservative decisions.

Figures 7 (a) and (b) show CLR evaluations when the mixture ratio of VCs is 1 : 2. VC1 has priority in (a) and VC2 has priority in (b). The horizontal axis denotes VP utilization, and the vertical axis denotes evaluated and simulated CLRs for the lower-priority class. The proposed CAC also gives accurate and conservative decisions.

Similarly, Figs. 8 (a) and (b) show CLR evaluations when the mixture ratio of VCs is 2 : 1. VC1 has priority in (a) and VC2 has priority in (b). The horizontal axis denotes VP utilization, and the vertical axis denotes evaluated and simulated CLRs for the lower-priority class. The proposed CAC also gives accurate and conservative decisions.

5.2 Calculation Time for CAC Decisions

This section shows the processing time for the proposed CAC.

First, we investigated the relationship between the number of iterations N in (25) and the accuracy of the evaluated CLR using numerical examples. It is necessary that X_N defined as (21) is positive. Therefore, $N \geq 4$ is required. For a small N, C_L defined as (20) becomes large and D is determined by C_L by (24). This means that different N's give different CLR evaluations with respect to the summation in (25) for a small N. Therefore, N is not a simple truncation parameter.

Figure 9 shows examples of the relationship between N and the evaluated CLR. The examples are 55, 45, and 35 VCs and have 10 Mbps of PCR, 2 Mbps of SCR and 50 cells of MBS. The capacity of VP is 150 Mbps and the capacity of the buffer is 500 cell

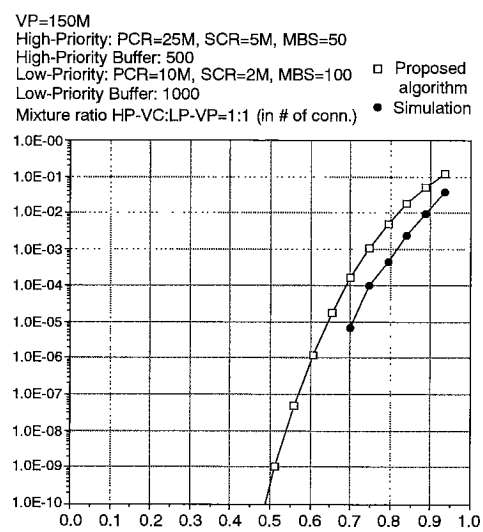

(a) VC1 has priority.

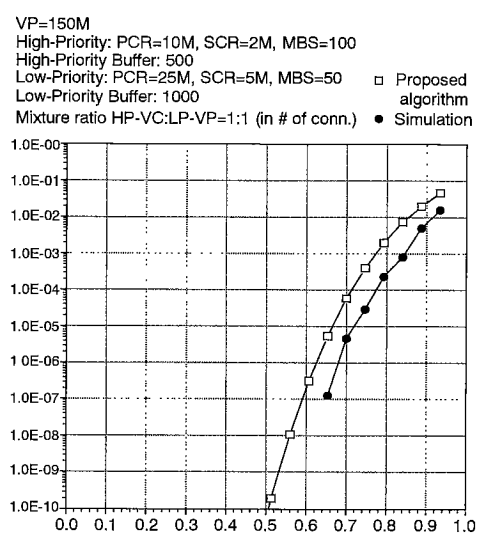

(b) VC2 has priority.

Fig. 6 Mixture ratio: 1 : 1 (in # of VCs).

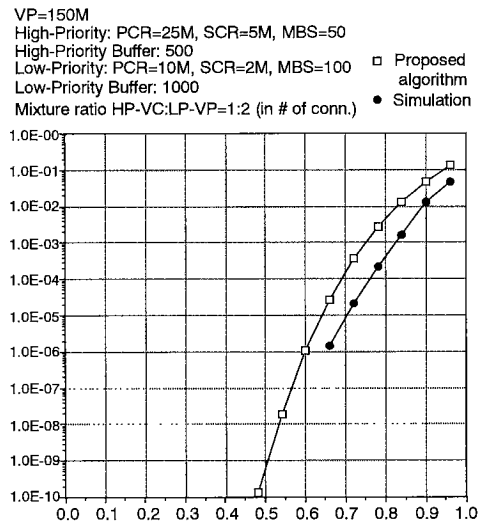

(a) VC1 has priority.

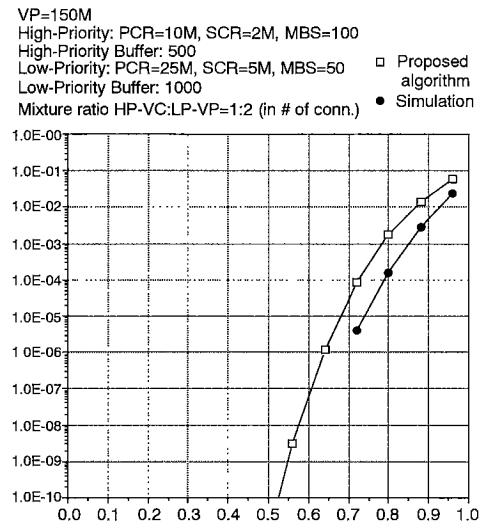

(b) VC2 has priority.

Fig. 7 Mixture ratio: 1:2 (in # of VCs).

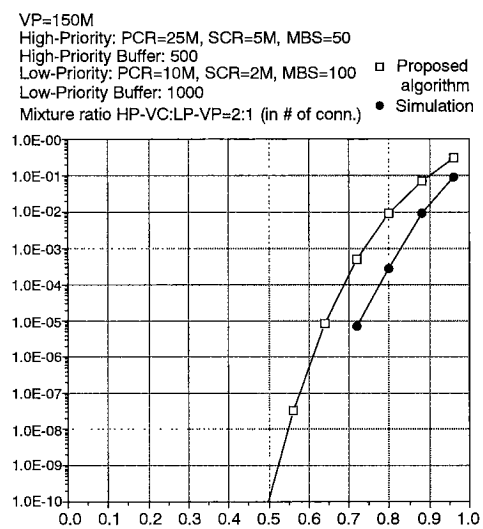

(a) VC1 has priority.

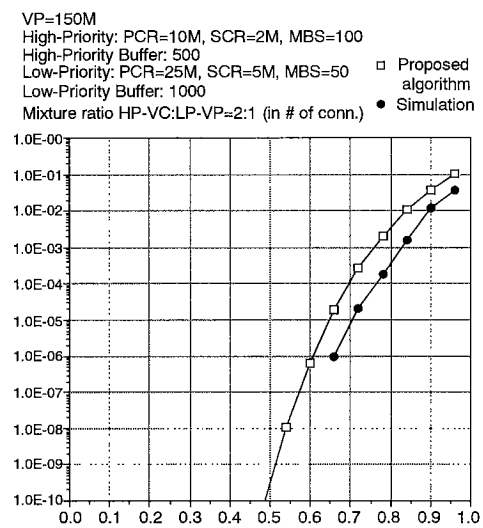

(b) VC2 has priority.

Fig. 8 Mixture ratio: 2:1 (in # of VCs).

places. The horizontal axis denotes the number of iterations N, and the vertical axis denotes the CLR evaluated by (25). Although N is small, the evaluated CLR is almost the same in the case of a large N. In applying the CLR evaluation algorithm to CAC, it gives sufficient accuracy when $N \geqq 10$.

Next, we assume that the call processor in SW is model 68040 with a floating-point co-processor, and its processing rate is 15 Mips. Table 2 shows the time for the CAC decision with respect to the new CBR, VBR-RT, and VBR-NRT VCs. These calculation times are independent of the number of VCs. This is a result of using the real-time CLR evaluation algorithm. The results show that the CAC process terminates within a few milliseconds, and real-time CAC for multiple service categories can be achieved using the proposed CAC.

Table 2 Calculation time for CAC decision.

the number of iterations N	10	20	30
CBR (msec)	1.2	1.6	2.1
VBR-RT (msec)	1.2	1.6	2.1
VBR-NRT (msec)	0.7	0.8	1.0

6. Conclusion

In this paper, we proposed a CAC scheme based on a real-time CLR evaluation algorithm. Since the CLR evaluation algorithm does not require convolution cal-

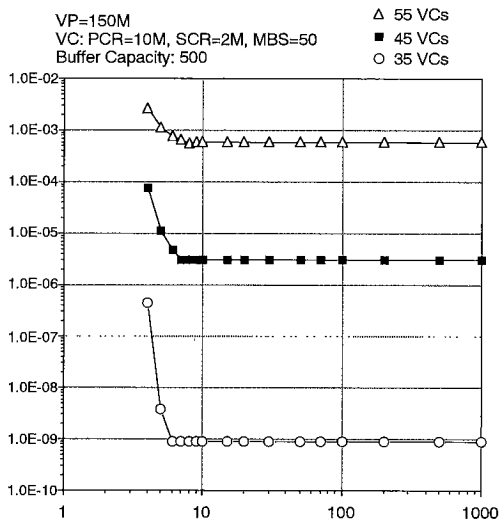

Fig. 9 The relationship between iterations N and the accuracy of CLR evaluation.

culations, the time necessary for CAC decision is short and independent of the number of VCs accommodated in the VP. In addition, it is also independent of the capacity of a cell buffer because of using the Allan variance of VP utilization. Moreover, the framework of the proposed CAC can support multiple service categories. Therefore, we can achieve real-time CAC for multiple service categories. Calculation time can still be reduced by using a higher-speed processor.

References

[1] The ATM Forum, "ATM User Network Interface Specification ver. 3.0," Prentice Hall, 1993.
[2] The ATM Forum, "ATM Forum Traffic Management Specification ver. 4.0," 95-0013R13, 1995.
[3] M. Aida and T. Kubo, "Efficient cell-loss ratio estimation for real-time CAC decisions," IEICE Trans. Commun., vol.E79-B, no.2, pp.108–115, 1996.
[4] M. Aida, "Congestion detection and CAC for ABR services using Allan variance," IEICE Trans. Commun., vol.E79-B, no.4, pp.540–549, 1996.
[5] M. Aida and M. Nakamura, "Realtime connection admission control for multiple service categories," Proc. ICCCN '96, Rockville, MD, 1996.
[6] M. Aida, "Realtime CAC scheme for multiple service categories including ABR with non-zero MCR," Proc. ATM '97 Workshop, Lisbon, Portugal, 1997.
[7] M. Aida, "Realtime cell-loss ratio evaluation using Allan variance," IEICE Trans. Commun., vol.E81-B, no.3, pp.683–688, 1998.
[8] D.W. Allan, "Statistics of atomic frequency standards," Proc. IEEE, vol.54, no.2, pp.221–230, 1966.
[9] H. Esaki, K. Iwamura, T. Komada, and T. Fukuda, "Connection admission control in ATM networks," IEICE Trans. Commun., vol.E77-B, no.1, pp.15–27, 1994.
[10] H. Yokoyama and H. Nakamura, "Dimensioning method of bandwidth requirement under priority control," IEICE Society Conf., E-7-108, 1997.
[11] W.V. Prestwitch, T.J. Kennet, and F.W. Kus, "The statistical properties of Allan variance," Can. J. Phys., vol.69, no.12, pp.1405–1415, 1991.
[12] H. Saito, "Teletraffic Technologies in ATM Networks," Artech House, Boston, 1994.
[13] H. Saito, "Call admission control using upper bound of cell loss probability," IEEE Trans. on Commun., vol.40, no.9, pp.1512–1521, 1992.
[14] H. Saito, "Hybrid connection admission control in ATM networks," Proc. ICC '92, 1992.
[15] H. Saito and K. Shiomoto, "Dynamic call admission control in ATM networks," IEEE JSAC, vol.9, no.7, pp.982–989, 1991.
[16] K. Shiomoto and S. Chaki, "Adaptive connection admission control using real-time traffic measurements in ATM networks," IEICE Trans. Commun., vol.E78-B, no.4, pp.458–464, 1995.

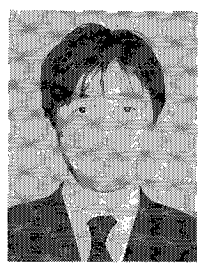

Masaki Aida received his B.S. and M.S. degrees in Theoretical Physics from St. Paul's University, Tokyo, Japan, in 1987 and 1989, respectively. Since he joined NTT Laboratories in 1989, he had been mainly engaged in research on traffic issues in ATM networks and computer communication networks until March 1998. He is currently a manager at Traffic Research Center, NTT Advanced Technology Corporation (NTT-AT). His current interests include traffic issues in communication systems. He received the Young Engineer Award of IEICE in 1996. Mr. Aida is a member of the Operations Research Society of Japan.